

Article

# Robust Assessment of Uncertain Freshwater Changes: The Case of Greece with Large Irrigation—and Climate-Driven Runoff Decrease

Georgia Destouni \*  and Carmen Prieto 

Department of Physical Geography, Bolin Centre for Climate Research and Navarino Environmental Observatory, Stockholm University, 10691 Stockholm, Sweden; carmen.prieto@natgeo.su.se

\* Correspondence: georgia.destouni@natgeo.su.se; Tel.: +46-8-164785

Received: 1 October 2018; Accepted: 8 November 2018; Published: 13 November 2018



**Abstract:** We develop a data-driven approach to robustly assess freshwater changes due to climate change and/or human irrigation developments by use of the overarching constraints of catchment water balance. This is applied to and tested in the high-uncertainty case of Greece for five nested catchments of different scales across the country and for freshwater changes from an early period (1930–1949) with small human influences on climate and irrigation to a recent period (1990–2009) with expected greater such influences. The results show more or less equal contributions from climatic decrease in precipitation and from human irrigation development to a considerable total decrease in runoff ( $R$ ) over Greece. This is on average  $-75 \pm 10$  mm/year and is greatest for the Ionian catchment in the west ( $-119 \pm 18$  mm/year) and the Peloponnese catchment in the south ( $-91 \pm 16$  mm/year). For evapotranspiration ( $ET$ ), a climate-driven decrease component and an irrigation-driven increase component have led to a net total increase of  $ET$  over Greece. This is on average  $26 \pm 7$  mm/year and is greatest for the Mainland catchment ( $29 \pm 7$  mm/year) and the Aegean catchment in the east ( $28 \pm 6$  mm/year). Overall, the resulting uncertainties in the water-balance constrained estimates of  $R$  and  $ET$  changes are smaller than the input data uncertainties.

**Keywords:** freshwater changes; irrigation; climate change; evapotranspiration; runoff; catchments; Greece

## 1. Introduction

Water is a peculiar liquid [1], critical for human existence and all life as we know it. Accurately understanding and being able to predict water conditions changes is among humanity's greatest needs and challenges [2,3]. This does not only apply to the major ocean part of Earth's hydrosphere but also to the essential freshwater on land. Freshwater changes on land interact with other Earth System changes, including changes in climate and in the landscape [4,5] and in both the ecosystems [6] and the societal systems [7–9] of the latter. In recognition of these interactions and critical open questions related to them, new hydrological research directions have developed such as the Panta Rhei community initiative [10] and the fields of ecohydrology [11] and sociohydrology [12].

The freshwater system itself includes various landscape manifestations and formations (streams, lakes, wetlands, water in biota, soil water, groundwater, glaciers, permafrost), with different aspects of variability and change interacting and propagating across them [13–16]. This propagation also involves interactions with different human uses of freshwater and structures for managing these, and all these freshwater interactions prevail and are organized within (the surface and subsurface parts of) hydrological catchments of different scales.

Furthermore, each hydrological catchment of any scale is subject to overarching water balance. In this, the total area-integrated water-fluxes of precipitation ( $P$ ) and evapotranspiration ( $ET$ ) and the

concurrent water-storage changes occurring over the catchment are balanced with each other and the total runoff flux ( $R$ ; area-normalized total discharge) from the catchment [17]. This emergent [18] catchment water balance is then also in simultaneous alignment with (i.e., both depends on and determines) and as such couples the different local water manifestations, formations, uses and management structures and the conditions of and changes in these over each catchment [19]. However, our ability to understand, interpret and predict these conditions and changes is currently fragmented among various research fields, associated with the different (liquid, frozen) freshwater manifestations and formations (e.g., surface water hydrology, hydrogeology, hydro-meteorology, ecohydrology, limnology, cryospheric science), or the different human uses of and management structures for freshwater (e.g., water resources engineering, hydraulic engineering, agricultural water management, urban water management, sociohydrology).

On the one hand, such freshwater fragmentation may be needed for in-depth process study and understanding. On the other hand, it may lead to important knowledge gaps and uncertainties between the fragments. Decrease of these gaps and uncertainties require ability to synthesize and jointly interpret various types of data, related to different freshwater aspects, which interact and coevolve with each other and other landscape and climate changes over hydrological catchments of different scales. For such synthesis and joint interpretation of different data for assessment of overall freshwater conditions and changes in a catchment of any scale, various studies have proposed [6,20] or indicated [4,5,19] that the constraints implied by catchment water balance may decrease the combined result uncertainties compared to the uncertainties associated with different underlying data and aspects.

In this paper, we put this indication to further testing for a case of particularly large underlying uncertainties [21]: Greece and five nested catchments of different scales across it. For these catchments, we investigate freshwater conditions and their changes over the time period 1930–2009, for which relevant data are available. Using the constraints implied by overarching water balance in each catchment, we develop, apply and test a general approach to synthesize, assess and interpret the available data for freshwater changes over the study period, the possible drivers of these changes and associated input-data and result uncertainties. Through the development and specific case quantification and testing of this approach, this study also outlines and uses advancements made in recent research on such long-term, large-scale freshwater changes.

## 2. Materials and Methods

### 2.1. Greece and Its Catchments

For several reasons, Greece is a relevant and useful case example for the present investigation. The country constitutes in itself the major part of a regional catchment draining into the Ionian and Aegean parts of the eastern Mediterranean Sea (Figure 1). Through Greece, this regional catchment is more or less peninsular and its long coastline facilitates selection of various nested coastal catchments of different scales within it, for comparative multi-catchment investigation using different parts of the available data for the total regional catchment.

Furthermore, previous comparative multi-catchment studies have shown that hydro-climatic changes and associated freshwater interactions with the atmosphere are subject to particularly large uncertainties in Greece [21]. These include: (a) uncertainties due to observation data limitations in terms of both temporal extent and spatial coverage across the country; and (b) climate model uncertainties for freshwater conditions, especially for model estimations of  $ET$  and, as a consequence, also of  $R$  and other related freshwater conditions in the Greek landscape for the reference period 1961–1990 [21]. These uncertainties make Greece a particularly important and useful case for investigating a possible robust methodology for catchment-wise data synthesis and interpretation and testing if the constraints implied by catchment water balance decrease the combined uncertainty effects for freshwater conditions and their changes.

Finally, in addition to climate change, Greece has undergone considerable agricultural irrigation developments over the study period 1930–2009, which is chosen due to availability of different types of relevant data for Greece over this period. Previous studies have reported such developments to be important drivers of freshwater changes in different parts of the world [7,8,17,22–24]. The occurrence of such developments over the study period in Greece contributes to making this a relevant case for studying freshwater changes and their interactions and co-evolution with such human-driven developments as well as with climate change.

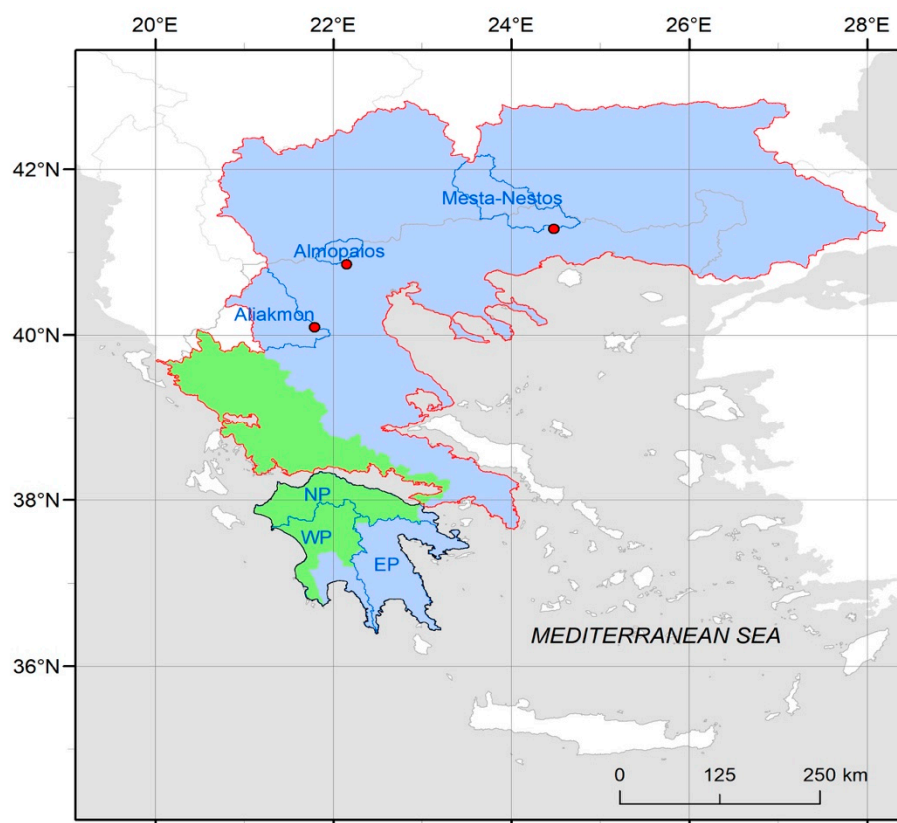


**Figure 1.** Location and extent of the nested study catchments. These include: the total regional catchment (coloured) and within it the catchments of: Mainland Greece (red outline) and Peloponnese (black outline); and of the Ionian Sea (green area) and the Aegean Sea (light blue area). Data-wise, the Mainland catchment includes three local catchments (blue outlines) with reasonable openly reported runoff data series. The Peloponnese catchment includes three water management districts and associated local catchments (blue outlines) of Northern Peloponnese (NP), Western Peloponnese (WP) and Eastern Peloponnese (EP) with available temporal average runoff and other freshwater data.

Overall, freshwater conditions, interactions and changes across Greece are here quantified and interpreted from the available reported data on hydro-climate and irrigated land-use and water-use for the period 1930–2009. To distinguish freshwater changes and associated uncertainties that may have been driven by the atmospheric climate change and/or the irrigation development occurring over Greece during this period, we compare long-term average conditions in relevant water-related variables between two 20-year sub-periods, 1930–1949 and 1990–2009, for five nested catchments of different scales (Figure 1). The two comparative sub-periods are chosen long enough to represent long-term average climate (and not just temporary weather) conditions and with as long time between them as possible for capturing freshwater changes from an early time with relatively small human influences on climate and irrigation to the recent time with expected much greater such influences.

With regard to the five catchments, the largest one is the total regional catchment (coloured in Figure 1; 178,984 km<sup>2</sup>) that includes the whole of Greece and drains into the eastern part of the

Mediterranean Sea through different coastline stretches. In addition to Greece (without its numerous islands, which are not considered in this study), this total catchment also includes some parts in the north that extend into the territories of the former Yugoslav Republic of Macedonia, Bulgaria, Turkey and a minor part of Serbia. This regional catchment is further divided into: the catchment of Mainland Greece (red outline in Figure 1; 157,550 km<sup>2</sup>) and that of Peloponnese (black outline in Figure 1; 21,434 km<sup>2</sup>); and the catchment draining into the Ionian Sea (green area in Figure 1; 31,958 km<sup>2</sup>) and that draining into the Aegean Sea (light blue area in Figure 1; 147,026 km<sup>2</sup>). These catchments are identified from reported watershed boundaries and associated vectorized river networks at 15 arc second by 15 arc second resolution [25].

Data-wise, the Mainland catchment includes three local catchments (blue outlines within the Mainland catchment in Figure 1) with reasonable openly reported data series of runoff (explaining further what is considered reasonable in the data section below). Moreover, the Peloponnese catchment includes three water management districts and associated local catchments (blue outlines within that catchment in Figure 1) of Northern Peloponnese (NP), Western Peloponnese (WP) and Eastern Peloponnese (EP), for which relevant temporal average runoff and other freshwater data are available (as described further below).

## 2.2. Hydro-Climatic Data

In general, open access data for the study region is limited in space and time. Long-term observations of the atmospheric variables surface temperature ( $T$ ) and  $P$  are readily available from global gridded databases like the CRU TS2.1 data set [26] and the more recently updated CRU TS3.10/CRU TS3.10.01 data sets at 0.5° grid-cell resolution [27]. However, for the water variables  $R$  and  $ET$  in the landscape, the spatio-temporal coverage of available regional data is much more limited.

Openly reported data in the Global Runoff Data Centre (GRDC) [28] show only three stream discharge stations in Greece with reasonable long-term annual average values for  $R$ . The reasonableness is judged by the long-term average  $R$  being smaller than the long-term average  $P$ , since equal or greater long-term average  $R$  (as found for other Greek discharge stations) implies unrealistic zero or negative long-term average  $ET = P - R$ . The reasons for the physically unreasonable discharge values reported for many stations in Greece are not known to us. For most of these discharge stations and the associated catchments, the annual aggregation of the  $R$  values (discharge divided by catchment area) implied by the reported discharge data in GRDC equals more or less the annual aggregation of the corresponding catchment-average  $P$  values in the CRU data; this indicates that the reported discharge data may not be independently measured but derived from catchment-average  $P$  data without accounting for the partitioning of the  $P$  water input between  $ET$  and  $R$ . At any rate, the three discharge stations with physically reasonable data and their local catchments are located in mainland Greece with the associated rivers being: Mesta-Nestos, Almpoiios and Aliakmon (Figure 1). Data from these stations in GRDC [28] have a maximum temporal extent of 24 successive years in the second half of the 20th century (Table 1).

For the Peloponnese, estimates representative of current long-term average  $R$  conditions are available from reports by the Greek Water Management Authority [29] for the three water management districts and associated local catchments NP, WP and EP (Figure 1). For these, average values of  $P$ ,  $R$  and  $ET$  are reported for different subcatchments, leading to the average  $ET/P$  ratios listed in Table 1.

**Table 1.** Data-based estimates of the ratio between long-term average evapotranspiration ( $ET$ ) and long-term average precipitation ( $P$ ) for the local catchments in mainland Greece and the river basin districts of Western, Northern and Eastern Peloponnese with relevant data availability. The term  $R$  represents long-term average runoff.

Catch-ment (Sta-tion)	Data in Mainland Greece					District	Data in Peloponnese				
	Area <sup>a</sup> (km <sup>2</sup> )	$P$ <sup>b</sup> (mm/year)	$R$ <sup>c</sup> (mm/year)	$ET$ <sup>g</sup> (mm/year)	$ET/P$		Area <sup>h</sup> (km <sup>2</sup> )	$R$ <sup>i</sup> (mm/year)	$ET$ <sup>i</sup> (mm/year)	$P_{eff}$ <sup>m</sup> (mm/year)	$ET/P_{eff}$
Mesta-Nestos (Teme-nos)	4948	666	283 <sup>d</sup>	383	0.57	Northern Peloponnese (NP)	6108	312 <sup>j</sup>	472 <sup>j</sup>	784	0.60
Almo-paios (Prof Ilias)	993	487	189 <sup>e</sup>	298	0.61	Western Peloponnese (WP)	7235	456 <sup>k</sup>	559 <sup>k</sup>	1015	0.55
Aliak-mon (Ila-rion)	5002	763	315 <sup>f</sup>	448	0.59	Eastern Peloponnese (EP)	8442	172 <sup>l</sup>	452 <sup>l</sup>	624	0.72

<sup>a</sup> Area calculated in ArcGIS. <sup>b</sup> Area-average  $P$  data over the years with runoff data from the gridded CRU TS2.1 data set [26]. <sup>c</sup> Temporal average over all years with available data from the GRDC [28]. <sup>d</sup> Monthly runoff data available for the period 1966–1989. <sup>e</sup> Monthly runoff data available for the period 1989–1994. <sup>f</sup> Monthly runoff data available for the period 1963–1987. <sup>g</sup>  $ET = P - R$ . <sup>h</sup> Greek Water Management Authority [29]. <sup>i</sup> Area-average of reported values from different subunits in management districts (as reported from the Greek Water Management Authority [29]). <sup>j</sup> Considered subunits: GR27 and GR28 (without the island subunit GR45) [29]. <sup>k</sup> Considered subunits: GR29 and GR32 [29]. <sup>l</sup> Considered subunits: GR30, GR31 and GR33 [29]. <sup>m</sup> Effective precipitation partitioning into the reported  $R$  and  $ET$  in the district:  $P_{eff} = R + ET$ .

2.3. Land- and Water-Use Data for Irrigation

Openly available information on irrigation rates and areas for Greece is not complete over either the whole investigated geographical space or the whole investigated time period. Two different types of such data are available: national irrigation data sets from statistics reported by the Organisation for Economic Co-operation and Development (OECD) [30,31]; and the global map of irrigated areas version 5.0 (GMIAv5.0) [32]. The national OECD data sets [30,31] contain statistics in terms of area that is actually irrigated ( $A_{ai}$ ) and total volume of water withdrawal for irrigation ( $I_{wvw}$ ) in Greece, especially from 1990 onwards (Figure 2). For earlier times, sporadic data on total irrigated area is provided by [33]. Furthermore, the global map of irrigation areas [32] represents the situation around year 2005 with spatial resolution of 5 arc minute by 5 arc minute (see Figure 3 for Greece).

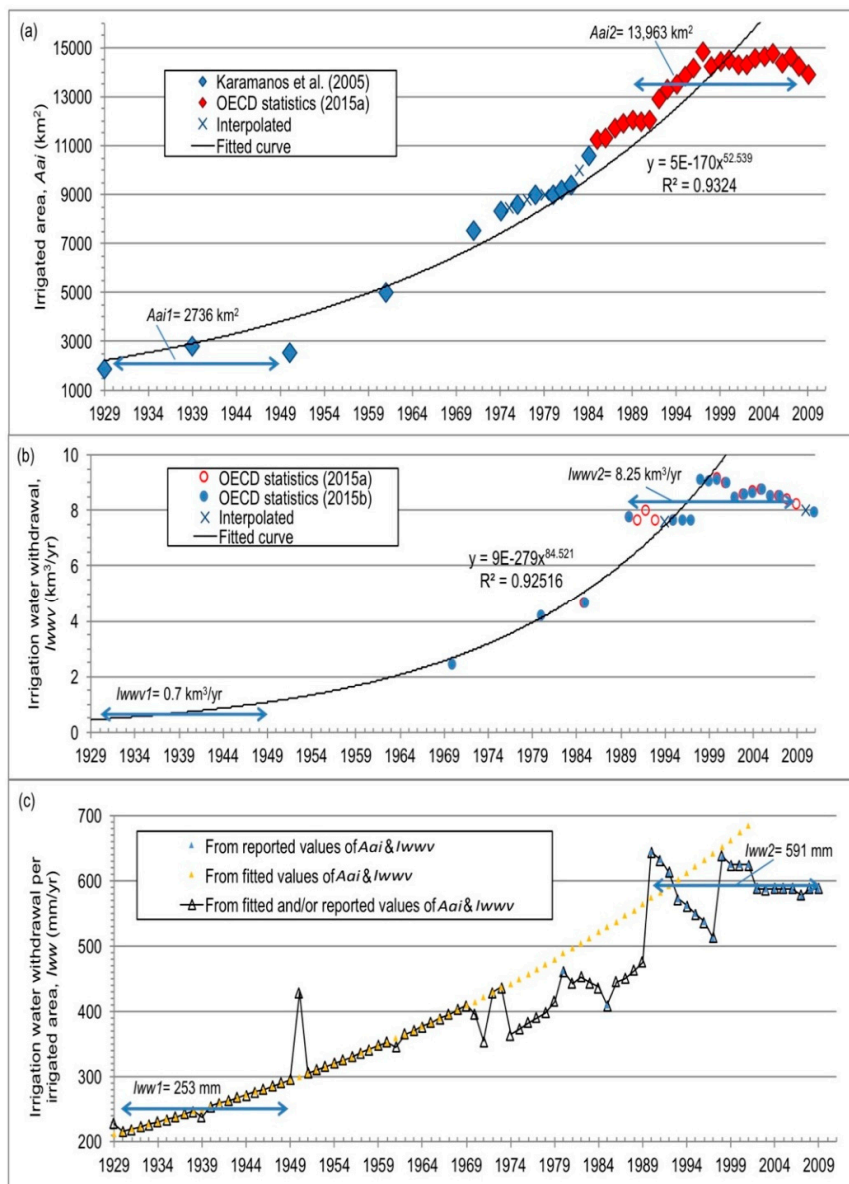


**Figure 2.** (a) Reported irrigated area,  $A_{ai}$ , in Greece, shown with the best power-law fit to the reported data. (b) Reported annual water withdrawal for irrigation,  $I_{wvw}$ , in Greece, shown with the best power-law fit to the reported data until year 2001, after which  $I_{wvw}$  conditions stabilize. (c) Irrigation water withdrawal per irrigated area,  $I_{ww} = I_{wvw} / A_{ai}$ , estimated from the reported and fitted data on  $A_{ai}$  and  $I_{wvw}$  in panels (a,b), respectively. The panels also show average variable values over the two 20-year sub-periods 1930–1949 and 1990–2009.

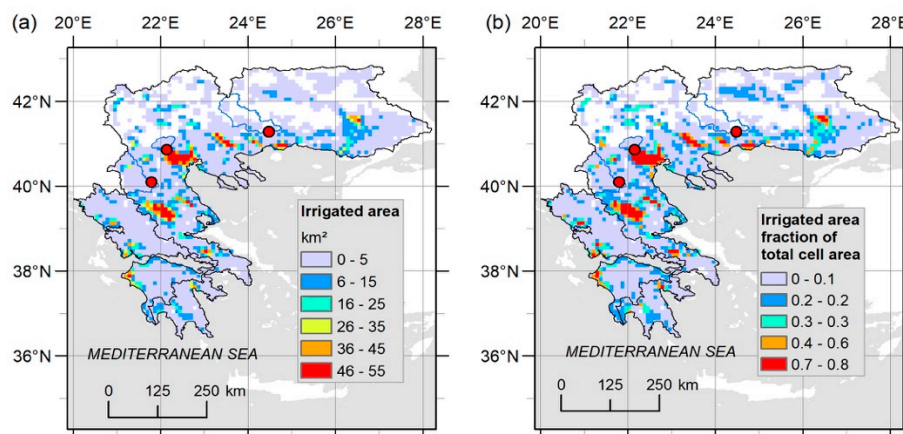


**Figure 3.** (a) Area actually irrigated within each grid cell in km<sup>2</sup>. (b) Irrigated area relative to total cell area. These maps are created from the global map of irrigation areas [32] and represent conditions in the recent period 1990–2009. In these maps, the Ionian and Aegean catchments are indicated by black outlines and the three local catchments in mainland Greece with reasonable runoff data time series are indicated by blue outlines.

#### 2.4. Assessing Freshwater Conditions and Changes

Temporal average  $T$  and  $P$  for the two comparative periods ( $T1$ ,  $P1$  for the early period 1930–1949 and  $T2$ ,  $P2$  for the recent period 1990–2009) are calculated from data on monthly  $P$  and  $T$ , as provided by the CRU TS 3.10/3.10.1 worldwide database extending over the period 1901–2009 [27]. Catchment-average values of these temporal averages are further quantified over all CRU grid cells with at least 34% of their area intersecting each considered catchment; Supplementary Figure S1 shows this CRU mask, used to extract catchment-average values of all analysed variables for each study catchment.

While period-average conditions for the atmospheric variables  $T$  and  $P$  can be calculated directly from available data series for the two comparative study periods, data on the average water fluxes in the landscape,  $ET$  and  $R$ , are not obtainable in this way for the earlier period 1930–1949. To estimate the early-period long-term average values of  $ET1$  and  $R1$  and the associated  $ET$  and  $R$  changes to the average values  $ET2$  and  $R2$  in the recent period 1990–2009, we start by evaluating the long-term average  $ET2$  value for 1990–2009 from the available  $P$  and  $R$  data for this period as  $ET2 = P2 - R2 = (ET2/P2) \times P2$ , based on the overarching long-term average water balance in each catchment. The data-given range of currently applicable  $ET/P$  values in Table 1 is calculated on this water-balance basis, following previous studies that have found [9,34] and assumed [5,7,8] long-term catchment-average changes in water storage to be near-zero over such long time periods.

To further estimate the change in average  $ET$  between the two 20-year periods, we follow the approach of previous studies [5,7,8] in estimating this total change as:

$$\Delta ET = ET2 - ET1 \approx \Delta ET_{clim} + \Delta ET_{irr}. \tag{1}$$

The second equality is approximate in assuming that total  $\Delta ET$  involves two main change components:  $\Delta ET_{clim}$  driven by climate change and  $\Delta ET_{irr}$  driven by irrigation changes. By evaluating these components,  $ET1$  can be estimated from Equation (1) as  $ET1 = ET2 - \Delta ET_{clim} - \Delta ET_{irr}$ .

Furthermore, from this quantification of  $ET1$ , the corresponding average  $R1$  can be consistently estimated as:

$$\begin{aligned} R1 &\approx P1 - ET1 = P1 - (ET2 - \Delta ET_{clim} - \Delta ET_{irr}) = P1 - ((P2 - R2) - \Delta ET_{clim} - \Delta ET_{irr}) \\ &= R2 - ((\Delta P - \Delta ET_{clim}) - \Delta ET_{irr}), \end{aligned} \tag{2}$$

with  $\Delta P = P2 - P1$  being the  $P$  change, and

$$\Delta R = R2 - R1 \approx (\Delta P - \Delta ET_{clim}) - \Delta ET_{irr} = \Delta R_{clim} + \Delta R_{irr} \quad (3)$$

being the total  $R$  change between the two periods. The climate-driven component of total  $\Delta R$  is thus quantified as  $\Delta R_{clim} = \Delta P - \Delta ET_{clim}$  and the corresponding irrigation-driven component is quantified as  $\Delta R_{irr} = -\Delta ET_{irr}$ .

To estimate the climate-driven change component  $\Delta ET_{clim}$ , we further relate the period-average temperature ( $T1, T2$ ) and precipitation ( $P1, P2$ ) to the corresponding average potential evapotranspiration ( $PET1, PET2$ ) based on the Langbein functional relationship [35] and further to corresponding  $ET$  conditions in each period ( $ET_{clim2}, ET_{clim1}$ ) based on the Turc functional relationship [36]. From these quantifications, the climate-driven  $ET$  change can be estimated as  $\Delta ET_{clim} = ET_{clim2} - ET_{clim1} = f(PET2, P2) - f(PET1, P1)$ . Alternative functional relationships for  $ET_{clim} = f(PET, P)$  may be used for this estimation but previous work has shown small differences in resulting changes of long-term catchment-average  $ET$  by use of alternative such functions [34].

Furthermore, to estimate the irrigation-driven change component  $\Delta ET_{irr} = ET_{irr2} - ET_{irr1}$ , we quantify the average irrigation water withdrawal per irrigated area in each period ( $Iww1, Iww2$ ) based on: the data and associated best-fit function for the temporal  $Iww$  evolution (Figure 2c); the area actually irrigated in absolute terms ( $Aai2$  from Figure 3a for recent period 1990–2009) and relative to total cell area ( $Aai_{rat2}$  from the map in Figure 3b for the recent period); and the assumption that more or less all water used for irrigation feeds back into the average  $ET$  over each period. The latter assumption is supported by previous studies of different irrigated areas of the world [17,22,23], as well as by recent findings of  $ET$  variations correlating well with concurrent, independently determined transpiration variations [16]. As irrigation is applied precisely for feeding into transpiration, it is reasonable to assume that it largely does so, or otherwise feeds into increased evaporation, either directly from soil water, or from potentially added surface water runoff; in any case, the applied irrigation water may be expected to largely feed into the total  $ET$  of each catchment. Moreover, a wide range of different possible  $Iww$  and  $Aai_{rat}$  evaluation scenarios are investigated (as described further in the following uncertainty analysis section) and may be expected to also cover uncertainty effects associated with varying parts of the irrigation water use ( $Iww$ ) and / or the relative irrigated catchment area ( $Aai_{rat}$ ) feeding into  $ET$  in each catchment. In general, based on these considerations and assumptions, an irrigation-driven part of total  $ET$  in each period is estimated as  $ET_{irr} \approx Iww \times Aai_{rat}$ . The difference between the resulting values of  $ET_{irr}$  for each of the two periods then provides the irrigation-driven change  $\Delta ET_{irr} = ET_{irr2} - ET_{irr1}$ .

In the absence of available data on the spatial distribution of irrigated area in the earlier period 1930–1949, we assume that the relative grid-cell irrigated area in that period ( $Aai_{rat1}$ ) is some fraction ( $\alpha_{irr}$ ) of the corresponding relative irrigation area in the recent period (i.e., that  $Aai_{rat1} = Aai_{rat2} \times \alpha_{irr}$ ). The fraction  $\alpha_{irr}$  is further assumed to be more or less the same for all grid cells and is estimated as such from the total irrigated area over Greece (Figure 3a) in the early period (total Greek  $Aai1$ ) relative to that in the recent period (total Greek  $Aai2$ ), that is, as  $\alpha_{irr} \approx (\text{total Greek } Aai1) / (\text{total Greek } Aai2)$ .

Table 2 summarizes a set of estimated input variables values, needed in the above-described calculations for each study catchment. Footnotes to Table 2 explain how these values are estimated and this evaluation is in the following referred to as the base case scenario for each catchment. This scenario is obtained using mean (or other relevant characteristic) values of the main input variables for each catchment and time period. In general, values that to some degree differ from those in the base case scenario may also be estimated for uncertain variables, depending on choices of data and assumptions made for the variable evaluation. To account for such evaluation uncertainty, we also consider possible alternative values of main uncertain variables, as explained further in the following section.

**Table 2.** Average variable values used in the base case scenario for each catchment and time period, 1930–1949 (*Per1*) and 1990–2009 (*Per2*). The terms *T*, *P*, *ET*, *I<sub>ww</sub>*, *A<sub>ai</sub>* and *A<sub>ai\_rat</sub>* represent temperature, precipitation, evapotranspiration, irrigation water withdrawal per irrigated area, irrigated area and ratio between *A<sub>ai</sub>* and total catchment area, respectively.

Catchments	Total		Mainland		Peloponnese		Ionian		Aegean	
Total area <sup>a</sup> (km <sup>2</sup> )	178,984		157,550		21,434		31,958		147,026	
Time Period	<i>Per1</i> <sup>b</sup>	<i>Per2</i> <sup>b</sup>	<i>Per1</i>	<i>Per2</i>	<i>Per1</i>	<i>Per2</i>	<i>Per1</i>	<i>Per2</i>	<i>Per1</i>	<i>Per2</i>
<i>T</i> <sup>c</sup> (°C)	12.1	12.4	11.7	12.1	15	14.8	14.4	14.4	11.6	12
<i>P</i> <sup>c</sup> (mm/year)	676	630	663	622	773	693	861	767	637	602
<i>ET/P</i> <sup>d</sup>		0.59		0.59		0.62		0.59		0.59
<i>I<sub>ww</sub></i> <sup>e</sup> (mm/year)	0.692/2736 = 253	8.25/13,963 = 591	253	591	253	591	253	591	253	591
<i>A<sub>ai</sub></i> (km <sup>2</sup> )	2736 <sup>e</sup>	11,046 <sup>f</sup>	2394 <sup>g</sup>	9665 <sup>f</sup>	342 <sup>g</sup>	1381 <sup>f</sup>	547 <sup>g</sup>	2255 <sup>f</sup>	2189 <sup>g</sup>	8791 <sup>f</sup>
<i>A<sub>ai_rat</sub></i>	0.015 <sup>h</sup>	11,046/178,984 = 0.062	0.015 <sup>h</sup>	9665/157,550 = 0.061	0.016 <sup>h</sup>	1381/21,434 = 0.064	0.017 <sup>h</sup>	2255/31,958 = 0.071	0.015 <sup>h</sup>	8791/147,026 = 0.06

<sup>a</sup> Spatial extent of each catchment. <sup>b</sup> *Per1*: 1930–1949, *Per2*: 1990–2009. <sup>c</sup> Spatio-temporal averages from the monthly CRU TS3.10.01 data set [27]. <sup>d</sup> Using the mean *ET/P* value from the three local catchments with data over mainland Greece and that from the Peloponnese local catchments over the Peloponnese. <sup>e</sup> From the national reported data on irrigated areas and irrigation water withdrawals [30,31] (Figure 2). <sup>f</sup> Spatial average values for each catchment with the area actually irrigated obtained from the GMIAv5.0 map dataset [32] (Figure 3). <sup>g</sup> Assuming that the ratio of areas actually irrigated in this catchment relative to that in the mainland Greece and the Peloponnese is more or less the same in 1930–1949 as in 1990–2009. <sup>h</sup> With *A<sub>ai\_rat1</sub>* estimated from:  $A_{ai\_rat1} = A_{ai\_rat2} \times a_{irr}$  and  $a_{irr} \approx A_{ai1}/A_{ai2} = 0.25$  in the base case scenario.

## 2.5. Uncertainty Analysis

For comparison with and uncertainty analysis of other possible variable values than those considered in the base case scenario (Table 2), we also evaluate alternative scenarios of uncertain variable values. Table 3 compares the base and the alternative scenarios and lists their variable value differences for the total regional catchment; Supplementary Table S1 does the same for the other four study catchments.

With regard to  $P$  data, the alternative scenarios outlined in Table 3 (named in the first and explained in the second column, in direct comparison with the base case) consider possible corrections for  $P$  undercatch bias [37], or for both undercatch and orographic biases [38]. Moreover, the  $ET/P$  ratio used for estimating average  $ET$  in the recent period 1990–2009 ranges from 0.55 to 0.72 among the local catchments with available data across Greece (Table 1). The base case scenario considers the mean value of  $ET/P$ , whereas two alternative  $ET/P$  scenarios consider corresponding minimum and maximum values (Table 3); the  $ET/P$  values are multiplied with  $P$  in each data grid cell to obtain grid-cell values of  $ET$  over each catchment.

Furthermore, considerable uncertainty about irrigation variables may stem from the estimation of water use (withdrawal) per irrigated area in the 1990–2009 period ( $Iww2$ ). For example, for the total regional catchment (Table 3),  $Iww2$  may be as large as 747 mm/year if the recent irrigated area in its calculation is estimated from the national reported irrigated area [30] ( $Aai2 = 13,963 \text{ km}^2$ ) instead of 591 mm/year in the base case scenario that estimates  $Iww2$  from GMIAv5.0 [32] ( $Aai2 = 11,046 \text{ km}^2$ ). The resulting uncertainty range of  $Iww2$  is then  $\pm 78 \text{ mm/year}$ .

With this uncertainty range given for  $Iww2$ , a corresponding uncertainty range of  $\pm 78 \text{ mm/year}$  may also be expected for  $Iww1$ , yielding an even wider uncertainty range for the temporal change in  $Iww$  by considering different possible combinations of  $Iww2$  and  $Iww1$  values in the base and alternative scenarios (as outlined in Table 3). Finally, also the value of the irrigation fraction  $\alpha_{irr} = Aai1/Aai2$  differs if the recent total irrigated area ( $Aai2$ ) is estimated from the GMIAv5.0 data [32] ( $11,046 \text{ km}^2$  for the regional catchment; base case scenario), or from the national reported data [30] ( $13,963 \text{ km}^2$  for the regional catchment; alternative scenario).

## 3. Results and Discussion

### 3.1. General Approach

A main result of this study is the general approach developed, used and tested for robustly assessing freshwater changes in terms of catchment-scale long-term average  $ET$  and  $R$ , driven by climate and landscape (here irrigation) developments from an earlier period (here 1930–1949) to recent conditions (here 1990–2009). Figure 4 illustrates schematically this principal approach, which is based on fundamental catchment water balance, aiming to constrain the result and uncertainty ranges of different possible variable evaluations. This approach provides a consistent flow-chart basis for corresponding quantitative assessments of freshwater changes in various comparative scenarios and catchment cases. Different scenarios may represent various possible variable evaluations from limited available observation data and the catchments may be of different scales and in different parts of the world.

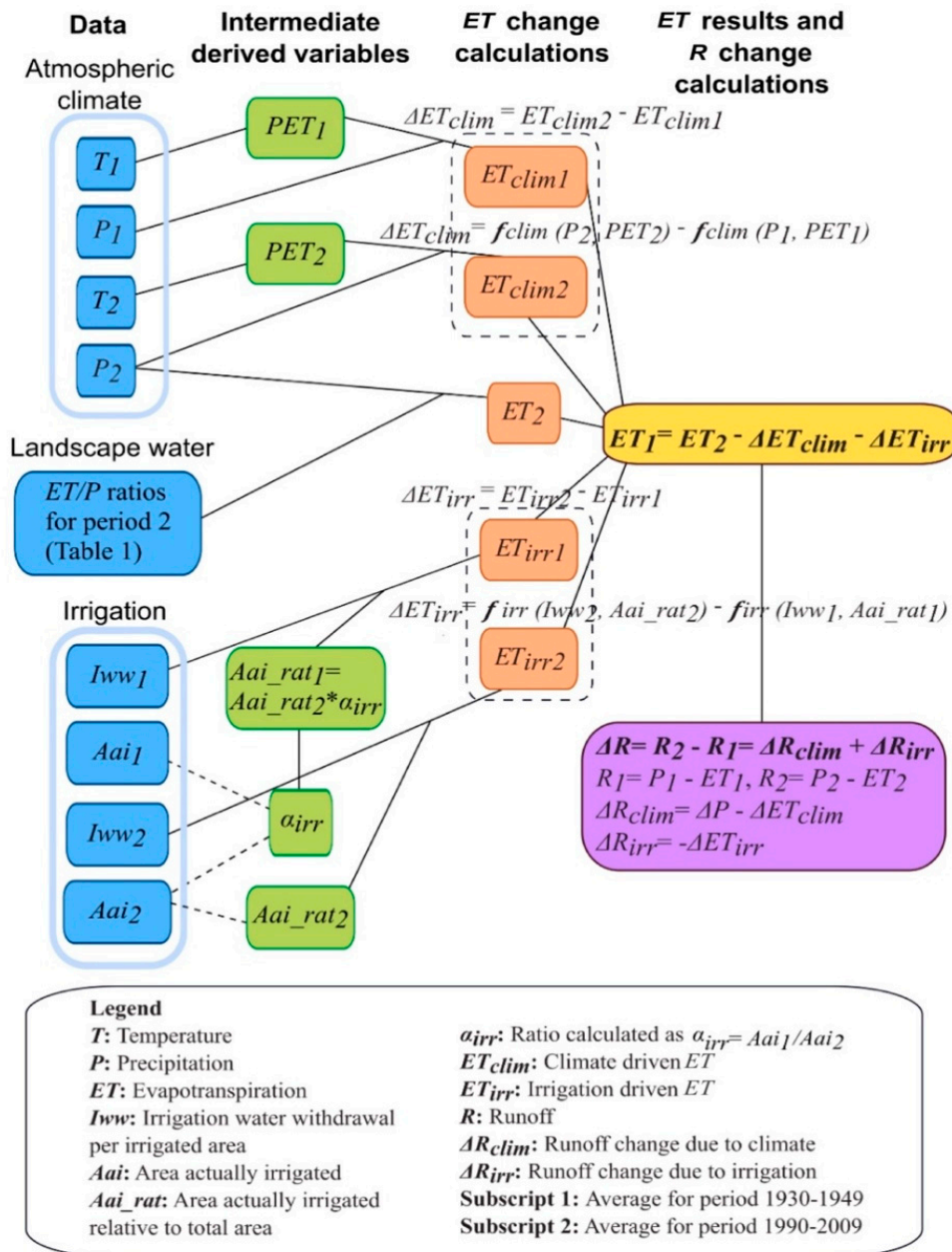


**Figure 4.** Schematic illustration of the approach developed and used to assess long-term average evapotranspiration ( $ET_1$ ) and runoff ( $R_1$ ) in an early 20-year period and associated changes ( $\Delta$ ) from this to a recent 20-year period. The sources and types of data used for the assessment in this study are exemplified for the base case scenario in the light blue boxes to the left, grouped as: atmospheric climate, landscape water and irrigation data. The variables extracted from the data are shown in the dark blue boxes. The green boxes show intermediate derived variables for estimating the different components of total  $ET$  change, as outlined in the red boxes and synthesized in the yellow box. The lilac box shows the final synthesis for estimating corresponding components and total change for  $R$ .

**Table 3.** The base case and alternative (Alt.) evaluation scenarios and their variations. Results are listed for the total regional catchment, with the terms  $P$ ,  $ET$ ,  $Iww$ ,  $\alpha irr$  and  $Per$  representing precipitation, evapotranspiration, irrigation water withdrawal per irrigated area, ratio  $Aai1/Aai2$  between irrigated area ( $Aai$ ) and time period. The latter is period 1 (1930–1949) or period 2 (1990–2009).

Total Regional Catchment			
Scenario	Variation	$Per1$	$Per2$
Base $P$	No correction of $P$ observation data (mm/year)	676	630
		−46	
Alt.1 $P$	Undercatch correction of $P$ observation data (mm/year)	734	686
		−48	
Alt.2 $P$	Undercatch and orographic correction of $P$ observation data (mm/year)	769	718
		−51	
Base $ET/P$	Mean $ET/P$		0.59
Alt.1 $ET/P$	Min $ET/P$		0.55
Alt.2 $ET/P$	Max $ET/P$		0.72
Base $Iww$	Mean $Iww1$ , Min $Iww2$ (mm/year)	253	591
		338	
Alt.1 $Iww$	Min $Iww1$ , Min $Iww2$ (mm/year)	175	591
		416	
Alt.2 $Iww$	Max $Iww1$ , Min $Iww2$ (mm/year)	331	591
		260	
Alt.3 $Iww$	Min $Iww1$ , Max $Iww2$ (mm/year)	175	747
		572	
Alt.4 $Iww$	Mean $Iww1$ , Max $Iww2$ (mm/year)	253	747
		494	
Alt.5 $Iww$	Max $Iww1$ , Max $Iww2$ (mm/year)	331	747
		416	
Base $\alpha irr$	Max $\alpha irr$	0.25	
Alt.1 $\alpha irr$	Min $\alpha irr$	0.20	

### 3.2. Freshwater Changes

Figure 5 shows the regional conditions and changes in the atmospheric variables  $T$  and  $P$  (top left in the general approach illustration, Figure 4), in terms of the spatial distribution of their temporal averages over the whole study period 1930–2009 (Figure 5a,b) and the changes in period-average  $T$  and  $P$  from 1930–1949 to 1990–2009 (Figure 5c,d). Spatially, long-term average  $T$  increases from a local range of around 7–11 °C in the north to around 15–18 °C in the south, while average  $P$  increases from a local range of around 460–800 mm/year in the east to around 800–1400 mm/year in the west. The corresponding changes also follow a north-south gradient for  $T$  and an east-west gradient for  $P$ . The temperature  $T$  increases in the cooler north and decreases in the warmer south (i.e., cool gets warmer and warm gets cooler), while  $P$  increases (or decreases the least) in the dry east and decreases (the most) in the wet west (i.e., dry gets wetter—or dries the least and wet gets drier—or dries the most).

Catchment-average results for  $T$  and  $P$  (Table 2, for the base case scenario) are consistent with the mapped grid-cell results (Figure 5) in showing that the most north-extending and coolest catchment (Aegean) has warmed the most (increase in average  $T$  of 0.4 °C) while the most southern and warmest catchment (Peloponnese) has cooled (decrease in average  $T$  of −0.2 °C). Moreover, while average  $P$

has decreased in all catchments, the most east-extending and driest catchment (Aegean) exhibits the smallest  $P$  decrease ( $-35$  mm/year) and the most western and wettest catchment (Ionian) exhibits the largest  $P$  decrease ( $-94$  mm/year).

Overall, the atmospheric hydro-climatic changes in  $T$  and  $P$  from 1930–1949 to 1990–2009 have driven most catchments (except the Peloponnese and Ionian) toward somewhat warmer conditions and all catchments toward drier conditions. Furthermore, these changes have decreased the variability range of average  $T$  and  $P$  among the nested catchments, from earlier ranges of  $3.4$  °C (from minimum  $11.5$  to maximum  $15$  °C) and  $224$  mm/year (from  $637$  to  $861$  mm/year) to recent ranges of  $2.8$  °C (from  $12$  to  $14.8$  °C) and  $145$  mm/year (from  $622$  to  $767$  mm/year), respectively.

With regard to irrigation, this has increased greatly in Greece in terms of all associated variables: irrigated area (Figure 2a) and amount of water used for irrigation in terms of absolute volume (Figure 2b) and per irrigated area (Figure 2c). These changes imply corresponding irrigation increases also in the different study catchments (Table 2). As a consequence of these human-driven irrigation developments, combined with the atmospheric hydro-climatic changes (Figure 5b), the long-term average values of the landscape hydro-climatic variables  $ET$  and  $R$  have also changed over Greece and in the different study catchments. Figures 6 and 7 illustrate the changes in  $ET$  and  $R$ , respectively, for all catchments. Further result details are listed in Table 4 for the total regional catchment; corresponding results for the other catchments are listed in Supplementary Table S2 for Mainland, Table S3 for Peloponnese, Table S4 for Ionian and Table S5 for Aegean.

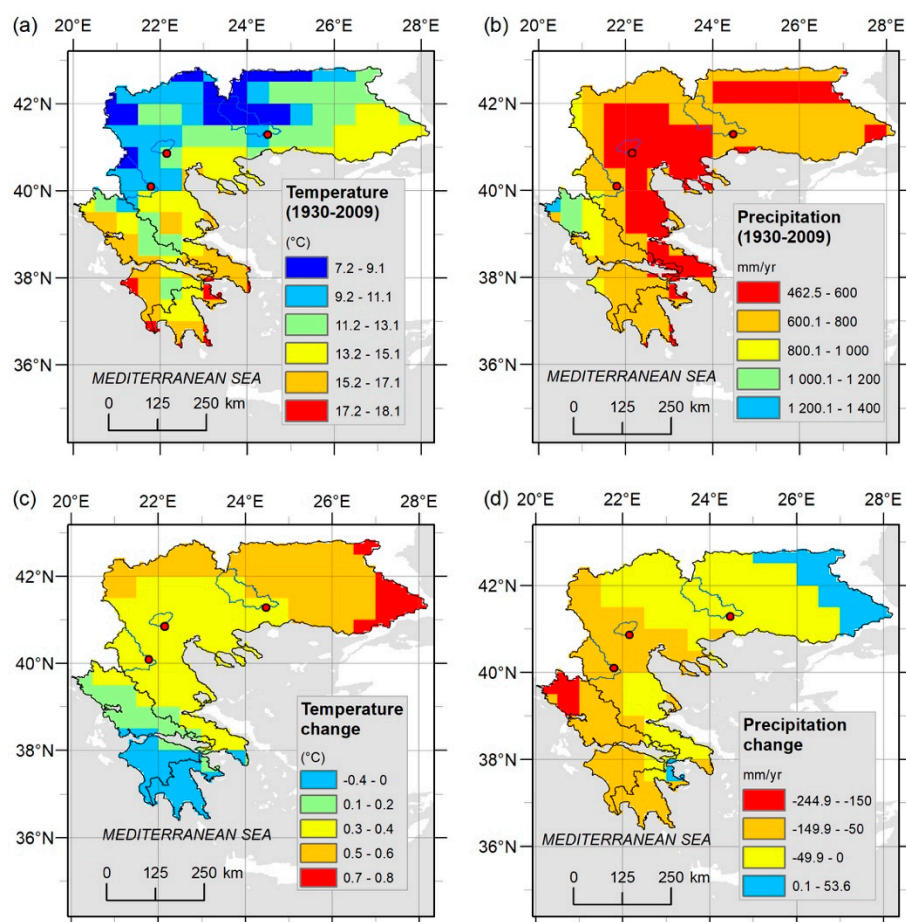


**Figure 5.** The spatial distribution of temporal average temperature (a) and precipitation (b) over the period 1930–2009 and corresponding period-average changes ((c,d), respectively) from the period 1930–1949 to the period 1990–2009. In these maps, the Ionian and Aegean catchments are indicated by black outlines and the three local catchments in mainland Greece with reasonable runoff data time series are indicated by blue outlines.

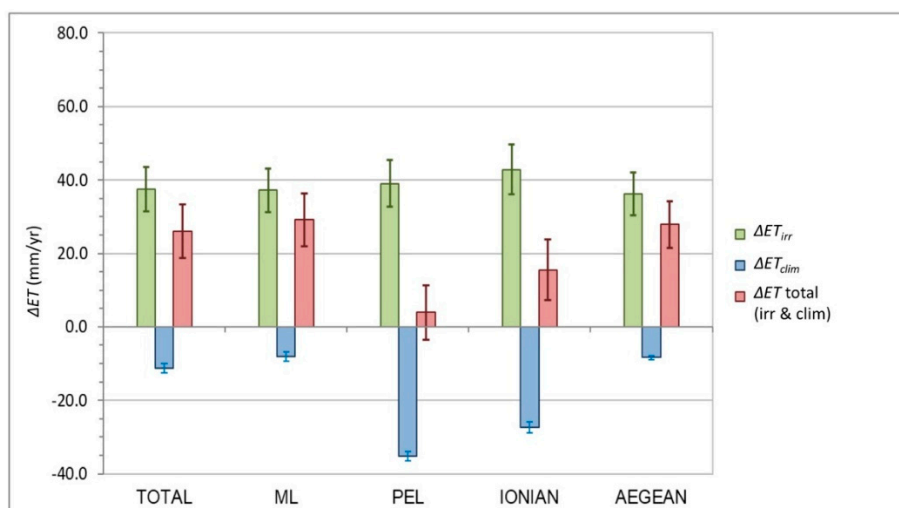


**Figure 6.** Evapotranspiration changes from 1930–1949 to 1990–2009 in total ( $\Delta ET$ ) and their climate ( $\Delta ET_{clim}$ ) and irrigation ( $\Delta ET_{irr}$ ) components. Main bars show mid-range results and error bars show the range of change estimates for different evaluation scenarios (Table 3 and Supplementary Table S1). Results are shown for the total regional catchment (TOTAL) and the nested Mainland (ML), Peloponnese (PEL), Ionian (IONIAN) and Aegean (AEGEAN) catchments.

**Table 4.** Freshwater changes and main uncertainty estimates for the total regional catchment. The terms  $P$ ,  $ET$  and  $R$  represent precipitation, evapotranspiration and runoff, respectively, while  $\Delta$  stands for change and subscript  $clim$  and  $irr$  indicate climate driven and irrigation driven change, respectively. Scenario definitions (Base, Alt.) are as given and explained in Table 3.

Type of Scenario and Uncertainty	$\Delta P$ (mm/year)	$\Delta ET_{clim}$ (mm/year)	$\Delta ET_{irr}$ (mm/year)	$\Delta ET$ (mm/year)	$\Delta R_{clim}$ (mm/year)	$\Delta R_{irr}$ (mm/year)	$\Delta R$ (mm/year)
$P$ scenarios $\pm$ Irrigation uncertainty	−46 (Base)	−12.5		24.9 $\pm$ 6	−33.5		−70.9 $\pm$ 6
	−48.4 (Alt. 1)	−11.5		25.9 $\pm$ 6	−36.9		−74.3 $\pm$ 6
	−51 (Alt. 2)	−10		27.4 $\pm$ 6	−41		−78.4 $\pm$ 6
Irrigation ( $I_{ww}$ ) scenarios $\pm P$ uncertainty			32.6 (Base)	21.3 $\pm$ 1.3		−32.6	−69.7 $\pm$ 3.8
			33.8 (Alt. 1)	22.5 $\pm$ 1.3		−33.8	−70.9 $\pm$ 3.8
			31.4 (Alt. 2)	20.1 $\pm$ 1.3		−31.4	−68.5 $\pm$ 3.8
			43.4 (Alt. 3)	32.1 $\pm$ 1.3		−43.4	−80.6 $\pm$ 3.8
			42.2 (Alt. 4)	30.9 $\pm$ 1.3		−42.2	−79.4 $\pm$ 3.8
		41 (Alt. 5)	29.7 $\pm$ 1.3		−41	−78.2 $\pm$ 3.8	
All scenarios $\pm$ Total uncertainty	−48.5 $\pm$ 2.5	−11.3 $\pm$ 1.3	37.4 $\pm$ 6	26.1 $\pm$ 7.3	−37.1 $\pm$ 3.8	−37.4 $\pm$ 6	−74.6 $\pm$ 9.8

Overall,  $ET$  has increased to some greater or lesser degree, while  $R$  has decreased considerably over all catchments. For  $ET$ , the irrigation developments have driven the largest change component  $\Delta ET_{irr}$  (overall increase of around 40 mm/year), while the climate-driven change  $\Delta ET_{clim}$  is in the opposite direction (decrease) and mostly of smaller absolute magnitude (around or less than 10 mm/year for the total, Mainland and Aegean catchments). For the Ionian and Peloponnese catchments, the absolute magnitude of the decrease  $\Delta ET_{clim}$  is relatively close to that of the increase  $\Delta ET_{irr}$ . As a consequence, the total net increase  $\Delta ET$  is relatively small in these two catchments (around 15 mm/year in the Ionian and 4 mm/year in the Peloponnese) and larger in the other catchments (around 25–30 mm/year).

The main reason for the relatively large decreases  $\Delta ET_{clim}$  of around −27 mm/year and −35 mm/year in the Ionian and the Peloponnese catchment, respectively, is that they are subject to the largest precipitation decreases  $\Delta P$  (of −94 mm/year and −80 mm/year). These are also combined with  $\Delta T$  conditions of zero warming (Ionian) or even cooling (of −0.2 °C in Peloponnese), which do not drive  $ET$  increase. A question to investigate in further climate-change research for this region is whether the generally large irrigation-driven  $ET$  increase ( $\Delta ET_{irr}$  component) and the additional latent

heat flux that this implies from the land surface to the atmosphere have contributed to significant local cooling of the land surface, thereby counteracting local warming effects of global climate change. This has been found in other irrigated regions of the world [17,23] and such irrigation-driven surface cooling would be consistent with the relatively small increases of local surface  $T$  over Greece, including the cooling and zero warming in the Peloponnese and Ionian catchments with the largest and second largest increase components  $\Delta ET_{irr}$ , respectively.

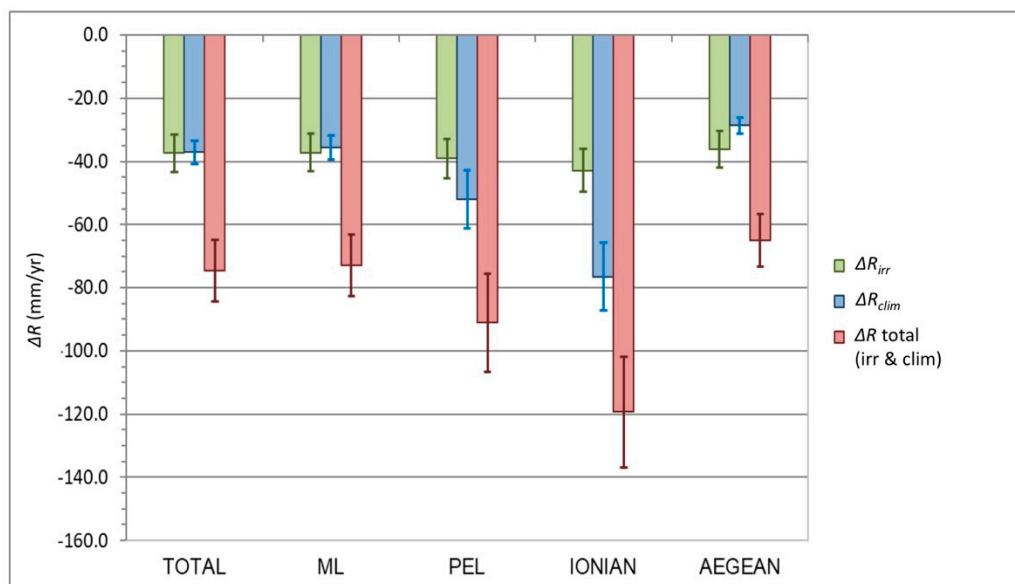


**Figure 7.** Runoff changes from 1930–1949 to 1990–2009 in total ( $\Delta R$ ) and their climate ( $\Delta R_{clim}$ ) and irrigation ( $\Delta R_{irr}$ ) components. Main bars show mid-range results and error bars show the range of change estimates for different evaluation scenarios (Table 3 and Supplementary Table S1). Results are shown for the total regional catchment (TOTAL) and the nested Mainland (ML), Peloponnese (PEL), Ionian (IONIAN) and Aegean (AEGEAN) catchments.

In contrast to  $ET$ , the climate and irrigation change components of  $\Delta R$  are both in the same direction, thus reinforcing each other and leading to considerable decrease in  $R$  across all catchments (Figure 7). In total,  $\Delta R$  is around:  $-75$  mm/year,  $-73$  mm/year and  $-65$  mm/year in the three largest catchments, total regional, Mainland and Aegean, respectively; and  $-91.1$  mm/year and  $-119$  mm/year in the two smallest catchments, Peloponnese and Ionian, respectively. The irrigation driven change component  $\Delta R_{irr} = -\Delta ET_{irr}$  (Equation (3)) has similar magnitude (decrease of around  $-40$  mm/year) across all catchments. In most catchments (total, Mainland, Aegean), the climate-driven change component  $\Delta R_{clim} = \Delta P - \Delta ET_{clim}$  (Equation (3)) is also a decrease of somewhat smaller magnitude (around  $-35$  to  $-30$  mm/year) than  $\Delta R_{irr}$ . However, in the Ionian and Peloponnese catchments, the decrease  $\Delta R_{clim}$  is larger (around  $-75$  mm/year and  $-50$  mm/year, respectively) than  $\Delta R_{irr}$ . Overall, the decrease  $\Delta R_{clim}$  is mainly due to the precipitation decrease  $\Delta P$  across all catchments.

The results of net total increase in average  $ET$  and decrease in average  $R$ , which for  $ET$  masks and for  $R$  exacerbates the decrease expected from only the observed atmospheric climate change (in  $T$  and  $P$ ), are consistent with corresponding results for other irrigated areas of the world. For example, in the Indian Mahanadi River catchment, draining into the Bay of Bengal, with decreased long-term average  $P$  by  $-60$  mm/year and increased irrigation water use by  $81$  mm/year (from 1901–1955 to 1956–2000), the average  $ET$  increased by around  $55$ – $70$  mm/year while the average  $R$  decreased by around  $-130$ – $-115$  mm/year [39]. Furthermore, in the case of the Aral Sea catchment (ASC),  $P$  increased by  $11$  mm/year and irrigation water use increased by  $23$  mm/year (from 1901–1950 to 1983–2002), while the average  $ET$  increased by  $15$  mm/year and the average  $R$  decreased by  $-28$  mm/year [39]. In both of these irrigation cases, as also found here for Greece, the irrigation development has led

to  $ET$  increase in spite of  $P$  decreasing (or to greater  $ET$  increase than the increase in  $P$  for ASC) and consequently to much greater decrease in  $R$  than the decrease in  $P$  (or to  $R$  decrease in spite of  $P$  increasing for ASC); in both cases, as in Greece, the large  $ET$  increase is also not explainable by just the observed warming (increase in average  $T$ ) over each catchment. A global study of  $ET$  changes around the world's land areas has also shown statistically that irrigated areas (and areas with dam and reservoir developments for meeting the irrigation and other increased water demands) have experienced significantly greater  $ET$  increases than other, more undisturbed land areas with regard to such human developments [8].

The irrigation-driven increases in  $ET$  imply greater losses of freshwater from the irrigated catchments. For most such catchments, these water losses are not compensated by corresponding increases in observed  $P$ , since the observed  $P$  changes (even combined with the observed  $T$  changes) cannot explain the total  $ET$  increases [8,39]. From its use for helping crops to survive dry season and drought conditions [16], the irrigation water adding to increased  $ET$  in an irrigated catchment is thus lost from that catchment and goes to feed other catchments or maybe even the sea. This leaves less freshwater for other uses in the irrigated catchment, such as for households, industry, energy generation and/or ecosystems. Water managers and decision makers need to understand the involved trade-offs and make conscious, informed choices for sustainably balancing freshwater uses among societal sectors and ecosystems. Further research is also needed to support such choices by investigating and revealing the implications of different development scenarios.

### 3.3. Uncertainty in Freshwater Changes

The error bars in Figures 6 and 7 show the uncertainty ranges of the estimated freshwater changes  $\Delta ET$  and  $\Delta R$ , as obtained in total from all considered uncertainty scenarios (Table 3, Supplementary Table S1). Table 4 lists further result details for the total regional catchment; corresponding results for the other catchments are listed in Supplementary Table S2 for Mainland, Table S3 for Peloponnese, Table S4 for Ionian and Table S5 for Aegean. In general, the total uncertainty range of  $\Delta ET$  ( $\pm 6$ – $8$  mm/year across all catchments) is smaller than that of  $\Delta R$ , which is also more variable among the catchments (from  $\pm 8$  for the Aegean up to  $\pm 18$  mm/year for the Peloponnese). Overall, these uncertainty ranges do not change the main results and implications discussed above based on the mean freshwater changes.

With regard to the investigated underlying uncertainties, the largest range is associated with the different scenarios of irrigation water use per irrigated area ( $I_{ww}$ ; Table 3). For the total regional catchment (Table 3), the estimated change in  $I_{ww}$  is on average 416 mm/year and the associated uncertainty range is  $\pm 156$  mm/year. In comparison, the resulting uncertainty ranges for this catchment are much smaller for both  $\Delta ET$  and  $\Delta R$ , at  $\pm 7$  and  $\pm 10$  mm/year, respectively. Similar results are obtained for this uncertainty propagation in all catchments, implying a major decrease in absolute range magnitude from that of underlying uncertainties (Table 3, Supplementary Table S1) to that of the total resulting  $\Delta ET$  and  $\Delta R$  uncertainties (Table 4, Supplementary Tables S2–S5).

Also in relative terms, the largest underlying uncertainty range is that for the  $I_{ww}$  change at  $\pm 38\%$ . For the decrease in  $R$  (Figure 7), the resulting relative uncertainty range is overall smaller: 13% for the total regional, Mainland and Aegean catchments (with mean  $\Delta R$  of  $-75$  mm/year,  $-73$  mm/year and  $-65$  mm/year, respectively); 15% for the Ionian catchment (with mean  $\Delta R$  of  $-119$  mm/year); and 17% for the Peloponnese catchment (with mean  $\Delta R$  of  $-91$  mm/year). For the increase in  $ET$  (Figure 6), the relative uncertainty range is larger and varies more among the catchments than that of  $\Delta R$ . Specifically, the relative  $\Delta ET$  range is:  $\pm 28\%$  for the total regional,  $\pm 25\%$  for the Mainland and  $\pm 23\%$  for the Aegean catchment (with mean  $\Delta ET$  of 26 mm/year, 29 mm/year and 28 mm/year, respectively);  $\pm 54\%$  for the Ionian catchment (with mean  $\Delta ET$  of 16 mm/year); and  $\pm 194\%$  for the Peloponnese catchment (with mean  $\Delta ET$  of just 4 mm/year).

In general, the largest contribution to the total  $\Delta ET$  range (of  $\pm 6$ – $8$  mm/year) stems from irrigation uncertainty ( $\pm 5$ – $6$  mm/year contribution; with additional  $\pm 1$  mm/year stemming from climate

uncertainty). For the total  $\Delta R$  range (of  $\pm 8$ – $18$  mm/year), the largest uncertainty contribution varies among catchments. For the Aegean, Mainland and total regional catchment, the largest contribution stems from irrigation uncertainty ( $\pm 6$ – $8$  mm/year contribution to their total  $\Delta R$  range of  $\pm 8$ – $10$  mm/year; with additional  $\pm 2$ – $4$  mm/year stemming from climate uncertainty, in which the main part is due to the  $\Delta P$  uncertainty of around  $\pm 2$  mm/year). In contrast, for the Ionian and Peloponnese catchments, the largest contribution stems from climate uncertainty ( $\pm 9$ – $11$  mm/year, in which the main part is due to the  $\Delta P$  uncertainty of  $\pm 7$ – $8$  mm/year, contributing to the total  $\Delta R$  range of  $\pm 16$ – $18$  mm/year; with  $\pm 6$ – $7$  mm/year stemming from irrigation uncertainty).

Across all catchments, the scenario combination with maximum *Iww1* and minimum *Iww2* (i.e., Alt. 2 *Iww* from Table 3) yields the lower  $\Delta ET$  and the upper  $\Delta R$  limit, while the opposite scenario combination with minimum *Iww1* and maximum *Iww2* (Alt. 3 *Iww*, Table 3) yields the upper  $\Delta ET$  and the lower  $\Delta R$  limit. The actual values of these limits depend also on the considered  $\Delta P$  scenario, with the undercatch correction (Alt 1 *P*, Table 3) and even more so the undercatch and orographic correction (Alt 2 *P*, Table 3) increasing the  $\Delta ET$  values and decreasing the  $\Delta R$  values compared to the base case scenario. The alternative scenarios for *ET/P* (Supplementary Table S6) and *airr* (not shown) do not significantly change the results compared to the Base case scenario.

#### 4. Conclusions

This paper has developed a general approach for synthesizing and jointly interpreting various types of data, related to different interacting and co-evolving drivers and aspects of freshwater change, subject to various degrees of uncertainty, over hydrological catchments of different scales. The application of this approach to the high-uncertainty case of Greece and its freshwater changes from 1930–1949 to 1990–2009, based on catchment water balance, provides support for an overall decrease in the combined uncertainties of resulting catchment-scale *ET* and *R* changes from the magnitude of the various underlying uncertainties.

For Greece, the study results are robust in showing that climate-driven *P* decrease and concurrent human-driven irrigation development from the first half of the 20th century to recent time have combined in driving considerable total decrease in *R* over the country. In the three largest study catchments (total regional, Mainland and Aegean), the total *R* decrease ranges from  $-65$  to  $-75$  mm/year  $\pm 13\%$ . This total *R* decrease is driven by the local irrigation development to more or less the same degree (possibly somewhat more but within the uncertainty range) as by climate change (predominantly decrease in *P*, with relatively small *T* increase over Greece and even decrease in Peloponnese). For the relatively small Ionian and Peloponnese catchments, the *R* decrease is up to  $-119$  mm/year  $\pm 15\%$  and  $-91$  mm/year  $\pm 17\%$ , respectively, due to the particularly large *P* decrease experienced in these catchments, combined with similar irrigation-driven *R* decrease as in the other catchments.

In each catchment, the irrigation-driven component of the total *R* decrease has largely fed a corresponding irrigation-driven component of *ET* increase. Recent results for water deficit propagation and partitioning over different parts of Europe [16] indicate that this *ET* increase likely represents increased transpiration, thereby contributing to support vegetation and crop status against the decreased *P* water input and the likely more frequent and/or more anomalous drought events that may be expected under such *P* decrease in Greece. Under these conditions of decreased *P* combined with relatively small *T* increase (or even *T* decrease), the atmospheric climate change drives *ET* decrease, that is, opposite change direction to the *ET* increase driven by irrigation. In net total, the irrigation-driven component dominates, such that total *ET* has increased (but less than *R* has decreased) over Greece, except in Peloponnese where the climate—and irrigation-driven components are more or less equal and total *ET* remains essentially unchanged.

**Supplementary Materials:** The following are available online at <http://www.mdpi.com/2073-4441/10/11/1645/s1>, Figure S1: Location and extent of CRU cells considered for each study catchment, Table S1: Base case and alternative (Alt.) quantification scenarios and their variations for different catchments, Table S2: Freshwater

changes and main uncertainty estimates for the Mainland catchment, Table S3: Freshwater changes and main uncertainty estimates for the Peloponnese catchment, Table S4: Freshwater changes and main uncertainty estimates for the Ionian catchment, Table S5: Freshwater changes and main uncertainty estimates for the Aegean catchment, Table S6: Evapotranspiration conditions and changes showing insignificant influence of choice of ET/P scenario (defined in main Table 3) for the example of the total regional catchment.

**Author Contributions:** G.D. conceived the study and analysis approach and wrote the paper. C.P. performed most analyses for the Figures and Tables and contributed to the writing.

**Funding:** This research was funded by The Swedish Research Council Formas, grant number 2016-02045.

**Conflicts of Interest:** The authors declare no conflict of interest.

## References

- Pettersson, L.G.M.; Henchman, R.H.; Nilsson, A. Water—The most anomalous liquid. *Chem. Rev.* **2016**, *116*, 7459–7462. [CrossRef] [PubMed]
- Nature Editorial. Get water governance on the global agenda. *Nature* **2016**, *540*, 169–170. [CrossRef]
- World Economic Forum. The Global Risks Report 2018. Available online: [http://www3.weforum.org/docs/WEF\\_GRR18\\_Report.pdf](http://www3.weforum.org/docs/WEF_GRR18_Report.pdf) (accessed on 30 September 2018).
- Bosson, E.; Sabel, U.; Gustafsson, L.G.; Sassner, M.; Destouni, G. Influences of shifts in climate, landscape and permafrost on terrestrial hydrology. *J. Geophys. Res. Atmos.* **2012**, *117*, D05120. [CrossRef]
- Jaramillo, F.; Destouni, G. Developing water change spectra and distinguishing change drivers worldwide. *Geophys. Res. Lett.* **2014**, *41*, 8377–8386. [CrossRef]
- Elmhagen, B.; Destouni, G.; Angerbjörn, A.; Borgström, S.; Boyd, E.; Cousins, S.A.O.; Dalén, L.; Ehrlén, J.; Ermold, M.; Hambäck, P.A.; et al. Interacting effects of change in climate, human population, land use and water use on biodiversity and ecosystem services. *Ecol. Soc.* **2015**, *20*, 23. [CrossRef]
- Destouni, G.; Jaramillo, F.; Prieto, C. Hydroclimatic shifts driven by human water use for food and energy production. *Nat. Clim. Chang.* **2013**, *3*, 213–217. [CrossRef]
- Jaramillo, F.; Destouni, G. Local flow regulation and irrigation raise global human water consumption and footprint. *Science* **2015**, *350*, 1248–1251. [CrossRef] [PubMed]
- Kalantari, Z.; Ferreira, C.S.S.; Walsh, R.P.D.; Ferreira, A.J.D.; Destouni, G. Urbanization development under climate change: Hydrological responses in a peri-urban Mediterranean catchment. *Land Degrad. Dev.* **2017**, *28*, 2207–2221. [CrossRef]
- Montanari, A.; Young, G.; Savenije, H.H.G.; Hughes, D.; Wagener, T.; Ren, L.L.; Koutsoyiannis, D.; Cudennec, C.; Toth, E.; Grimaldi, S.; et al. “Panta Rhei—Everything Flows”: Change in hydrology and society—The IAHS Scientific Decade 2013–2022. *Hydrol. Sci. J.* **2013**, *58*, 1256–1275. [CrossRef]
- Smettem, K.R.J. Welcome address for the new ‘Ecohydrology’ Journal. *Ecohydrology* **2008**, *1*, 1–2. [CrossRef]
- Sivapalan, M.; Savenije, H.H.G.; Blöschl, G. Socio-hydrology: A new science of people and water. *Hydrol. Process* **2012**, *26*, 1270–1276. [CrossRef]
- Karlsson, J.M.; Lyon, S.W.; Destouni, G. Thermokarst lake, hydrological flow and water balance indicators of permafrost change in Western Siberia. *J. Hydrol.* **2012**, *464–465*, 459–466. [CrossRef]
- Berghuijs, W.R.; Woods, R.A.; Hrachowitz, M. A precipitation shift from snow towards rain leads to a decrease in streamflow. *Nat. Clim. Chang.* **2014**, *4*, 583–586. [CrossRef]
- Karlsson, M.J.; Jaramillo, F.; Destouni, G. Hydro-climatic and lake change patterns in Arctic permafrost and non-permafrost areas. *J. Hydrol.* **2015**, *529*, 134–145. [CrossRef]
- Orth, R.; Destouni, G. Drought reduces blue-water fluxes more strongly than green-water fluxes in Europe. *Nat. Commun.* **2018**, *9*, 3602. [CrossRef] [PubMed]
- Destouni, G.; Asokan, S.M.; Jarsjö, J. Inland hydro-climatic interaction: Effects of human water use on regional climate. *Geophys. Res. Lett.* **2010**, *37*, L18402. [CrossRef]
- De Haan, J. How emergence arises. *Ecol. Complex.* **2006**, *3*, 293–301. [CrossRef]
- Baresel, C.; Destouni, G. Novel quantification of coupled natural and cross-sectoral water and nutrient/pollutant flows for environmental management. *Environ. Sci. Technol.* **2005**, *39*, 6182–6190. [CrossRef] [PubMed]

20. Thorslund, J.; Jarsjo, J.; Jaramillo, F.; Jawitz, J.W.; Manzoni, S.; Basu, N.B.; Chalov, S.R.; Cohen, M.J.; Creed, I.F.; Goldenberg, R.; et al. Wetlands as large-scale nature-based solutions: Status and challenges for research, engineering and management. *Ecol. Eng.* **2017**, *108 Pt B*, 489–497. [CrossRef]
21. Bring, A.; Asokan, S.M.; Jaramillo, F.; Jarsjö, J.; Levi, L.; Pietroni, J.; Prieto, C.; Rogberg, P.; Destouni, G. Implications of freshwater flux data from the CMIP5 multi-model output across a set of Northern Hemisphere drainage basins. *Earth's Future* **2015**, *3*, 206–217. [CrossRef]
22. Jarsjö, J.; Asokan, S.M.; Prieto, C.; Bring, A.; Destouni, G. Hydrological responses to climate change conditioned by historic alterations of land-use and water-use. *Hydrol. Earth Syst. Sci.* **2012**, *16*, 1335–1347. [CrossRef]
23. Asokan, S.M.; Rogberg, P.; Bring, A.; Jarsjö, J.; Destouni, G. Climate model performance and change projection for freshwater fluxes: Comparison for irrigated areas in Central and South Asia. *J. Hydrol. Reg. Stud.* **2016**, *5*, 48–65. [CrossRef]
24. Jaramillo, F.; Destouni, G. Comment on “Planetary boundaries: Guiding human development on a changing planet”. *Science* **2017**, *348*, 1217. [CrossRef] [PubMed]
25. Lehner, B.; Verdin, K.; Jarvis, A. HydroSHEDS Technical Documentation. World Wildlife Fund US, Washington, D.C. Available online: <http://hydrosheds.cr.usgs.gov> (accessed on 24 April 2013).
26. Mitchell, T.D.; Jones, P.D. An improved method of constructing a database of monthly climate observations and associated high-resolution grids. *Int. J. Clim.* **2005**, *25*, 693–712. [CrossRef]
27. Harris, I.; Jones, P.D.; Osborn, T.J.; Lister, D.H. Updated high-resolution grids of monthly climatic observations—the CRU TS3.10 Dataset. *Int. J. Clim.* **2014**, *34*, 623–642. [CrossRef]
28. GRDC. Global Runoff Data Centre, Koblenz, Germany. Available online: <http://www.bafg.de> (accessed on 3 June 2013).
29. Greek Water Management Authority. *Water Management Plan for the Greek River Basin Districts (GR06)*; Greek Water Management Authority: Athens, Greece, 2013; Volume 2.
30. Organisation for Economic Co-operation and Development, Statistics. Extracted by Selecting Environmental Indicators for Agriculture, Environmental Performance of Agriculture 2013, Water Resources, Environmental Indicator: Irrigation, Irrigated Areas (ha) and Irrigation Freshwater Withdrawals (million m<sup>3</sup>). Available online: <http://stats.oecd.org/Index.aspx#> (accessed on 4 May 2015).
31. Organisation for Economic Co-Operation and Development, Statistics. Extracted by Selecting Environment\Water\Freshwater Abstractions (million m<sup>3</sup>). Variable: Irrigation\Total freshwater for Greece. Available online: <http://stats.oecd.org/Index.aspx#> (accessed on 4 May 2015).
32. Siebert, S.; Henrich, V.; Frenken, K.; Burke, J. *Global Map of Irrigation Areas Version 5*; Rheinische Friedrich-Wilhelms-University: Bonn, Germany; Food and Agriculture Organization of the United Nations: Rome, Italy, 2013.
33. Karamanos, A.; Aggelides, S.; Londra, P. *Irrigation Systems Performance in Greece*; Options Méditerranéennes, Series B, No. 52; CIHEAM: Bari, Italy, 2005.
34. Jaramillo, F.; Prieto, C.; Lyon, S.W.; Destouni, G. Multimethod assessment of evapotranspiration shifts due to non-irrigated agricultural development in Sweden. *J. Hydrol.* **2013**, *484*, 55–62. [CrossRef]
35. Langbein, W.B. Annual runoff in the United States. *Geol. Surv. Circ.* **1949**, *52*. [CrossRef]
36. Turc, L. “The water balance of soils”, relation between precipitation, evaporation and flow. *Ann. Agron.* **1954**, *5*, 491–569.
37. Adam, J.C.; Lettenmaier, D.P. Adjustment of global gridded precipitation for systematic bias. *J. Geophys. Res.* **2003**, *108*, 1–14. [CrossRef]
38. Adam, J.C.; Clark, E.A.; Lettenmaier, D.P.; Wood, E.F. Correction of global precipitation products for orographic effects. *J. Clim.* **2006**, *19*, 15–38. [CrossRef]
39. Asokan, S.M.; Destouni, G. Irrigation effects on hydro-climatic change: Basin-wise water balance-constrained quantification and cross-regional comparison. *Surv. Geophys.* **2014**, *35*, 879–895. [CrossRef]

